Hydrogen-Bubble-Propelled Zinc-Based Microrockets in Strongly Acidic Media

3 AUTHORS, INCLUDING:

Wei Gao
University of California, Berkeley
59 PUBLICATIONS **1,815** CITATIONS

SEE PROFILE

Aysegul Uygun Oksuz
T.C. Süleyman Demirel Üniversitesi
62 PUBLICATIONS **531** CITATIONS

SEE PROFILE

Hydrogen-Bubble-Propelled Zinc-Based Microrockets in Strongly Acidic Media

Wei Gao, Aysegul Uygun, and Joseph Wang*

Department of Nanoengineering, University of California, San Diego, La Jolla, California 92093, United States

S *Supporting Information*

ABSTRACT: Tubular polyaniline (PANI)/Zn micro-rockets are described that display effective autonomous motion in extreme acidic environments, without any additional chemical fuel. These acid-driven hydrogen-bubble-propelled microrockets have been electrosynthesized using the conical polycarbonate template. The effective propulsion in acidic media reflects the continuous thrust of hydrogen bubbles generated by the spontaneous redox reaction occurring at the inner Zn surface. The propulsion characteristics of PANI/Zn microrockets in different acids and in human serum are described. The observed speed–pH dependence holds promise for sensitive pH measurements in extreme acidic environments. The new microrockets display an ultrafast propulsion (as high as 100 body lengths/s) along with attractive capabilities including guided movement and directed cargo transport. Such acid-driven microtubular rockets offer considerable potential for diverse biomedical and industrial applications.

D esigning and powering new synthetic nano-/microscale motors represent a major challenge and opportunity. Considerable efforts have thus been devoted to the preparation of efficient nanomotors propelled by different mechanisms.[1−12] Particular attention has been given to chemically powered catalytic micro-/nanomotors, based on different compositions and structures, that are capable of moving autonomously in the presence of hydrogen peroxide fuel.[13−18] Among these catalytic motors, self-propelled tubular microbots are particularly attractive for practical biomedical applications.[18−22] The oxygen-bubble propulsion mechanism of such tubular microbots leads to efficient propulsion in relevant biological fluids and high-ionic-strength media, as desired for diverse practical applications ranging from directed cargo transport in microchips[23,24] to isolation of target biomaterials from body fluids.[25−28] A simplified template electrosynthesis of highly efficient, ultrafast, and small polyaniline (PANI)/Pt bilayer microtube engines was reported recently.[29] However, the requirement of high concentration of the hydrogen peroxide fuel has greatly hindered practical applications of these and other catalytically propelled micro-/nanomotors. Sen's group developed recently a bisegment Pt/Cu nanowire motor that uses bromine or iodine fuels, instead of hydrogen peroxide.[30] Yet, owing to its self-electrophoresis propulsion mechanism, such nanowire motor cannot be operate in high ionic strength environments.[31]

This Communication reports on a new PANI/Zn micro-rocket that propels autonomously and efficiently in extreme acidic environments without additional fuels. Such acid-driven microtubular rocket relies on a bubble propulsion mechanism associated with the continuous thrust of hydrogen bubbles generated at the inner zinc layer (Figure 1a), analogous to that
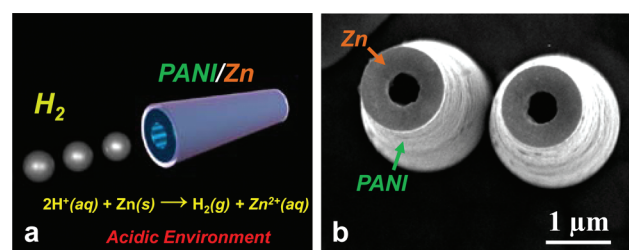
Figure 1. Acid-driven PANI-Zn microrocket: (a) schematic of motion in an acidic environment; (b) SEM images of the top view of two PANI-Zn microtubes (prepared using a membrane with 2 μm diameter pores).

of oxygen-bubble-propelled catalytic microengines.[18−22] When the new PANI/Zn bilayer microrockets are immersed in a strongly acidic medium, a spontaneous redox reaction—involving the Zn oxidation along with generation of hydrogen bubbles—occurs on their inner Zn surface:

$$\text{Zn(s)} + 2\text{H}^+(\text{aq}) \rightarrow \text{Zn}^{2+}(\text{aq}) + \text{H}_2(\text{g}) \qquad E° = 0.76\,\text{V} \qquad (1)$$
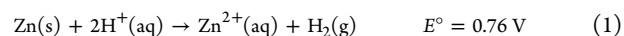
leading to an ultrafast propulsion that can exceed 100 body lengths/s. Zinc has a more negative redox potential than hydrogen and thus promotes hydrogen gas evolution;[32,33] hence, it has been widely used for producing hydrogen energy.[34,35] Other metals (e.g. Fe, Co, Sn, Pb) with a more negative redox potential than hydrogen were tested but displayed a much weaker bubble thrust. Alkali metals (e.g. Li, K), which can also lead to efficient hydrogen evolution, cannot be electrodeposited and are too reactive for a safe operation. Zn, in contrast, is an attractive candidate for the microrocket inner layer as it is a biocompatible "green" nutrient trace element, vital for many body functions and metabolic and enzymatic processes,[36] that can be readily electrodeposited and offers an efficient and safe acid-driven propulsion.

Strongly acidic environments can be found everywhere in our life, from diverse industrial processes to our own human stomach. Autonomous microrocket movement in such acidic

media can thus lead to diverse biomedical or industrial applications and hence greatly expand the scope of applications of nano-/microscale motors compared to common peroxide-driven catalytic micro-/nanomotors. As will be illustrated below, the new acid-driven PANI/Zn microrockets can also serve as an attractive platform for sensitive pH measurements in these extreme environments.

To take advantage of the Zn-induced hydrogen generation for the new bubble-propelled motors, PANI/Zn bilayer microtubes have been fabricated within a Cyclopore polycarbonate template containing microconical pores. The outer PANI tube was prepared in a manner analogous to that reported recently for preparing oxygen-bubble-propelled PANI/Pt microrockets.[29] Subsequently, a zinc layer was deposited galvanostatically within the PANI layer using an 80 g L^{-1} ZnSO$_4$/20 g L^{-1} H$_3$BO$_3$ solution (buffered to pH 2.5 with sulfuric acid). Figure 1b displays SEM images of the PANI/Zn bilayer microtube rockets prepared electrochemically using the 2 μm membrane (2 μm refers to the diameter of the bigger opening of the conical pore). The resulting microrockets are ~10 μm long, have a front inner opening diameter of ~350 nm and a front outer diameter of ~1.2 μm, and include a ~150 nm thick PANI outer layer and a ~300 nm Zn inner layer. The presence of carbon and zinc in the resulting bilayer microtubes was confirmed by EDX mapping analysis (not shown).

Figure 2 displays time-lapse images, taken from SI Video 1, for the movement of the PANI/Zn microrocket over a 360 ms
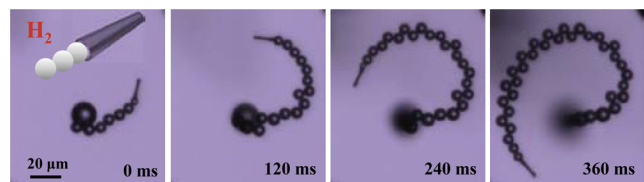
Figure 2. Acid-powered microengine: time-lapse images of the propulsion of a PANI/Zn microrocket (2 μm diameter) at 0, 120, 240, and 360 ms, respectively. Medium, 1 M HCl solution containing 1.67% Triton X-100.

period at 120 ms intervals in a strongly acidic environment (1.0 M HCl, pH 0). These images illustrate a tail of hydrogen microbubbles (~4−5 μm in diameter) generated on the inner Zn surface and released from the rear large-opening side of the microtube at a rate of 75 bubbles/s. The microrocket is self-propelled at an ultrafast speed over 500 μm/s, which corresponds to a relative speed of nearly 50 body lengths/s. Such speed is stable during the motor lifetime, except for an initial (~1 s) acceleration after immersion in the acid solution that reflects the increased inner diameter.

The speed of the acid-driven PANI/Zn microrocket is strongly dependent on the acid concentration. Figure 3 illustrates the influence of the pH and HCl concentration on the speed of microrockets with 2 and 5 μm diameters (black and red curves, respectively). As expected, both microrockets display their highest speed using the highest (1.6 M) acid concentration tested (corresponding to pH −0.2). For the 2 μm rocket, the speed decreases gradually from 650 μm/s (at pH −0.2) to 550 μm/s (at pH 0.0), then more rapidly to 300 μm/s (at pH 0.2), and subsequently slowly to 8 μm/s (at pH 1.0). The 5 μm diameter microrocket displays a similar trend, along with a higher initial speed and slightly wider pH range. This microrocket achieves an ultrafast speed of 1050 μm/s
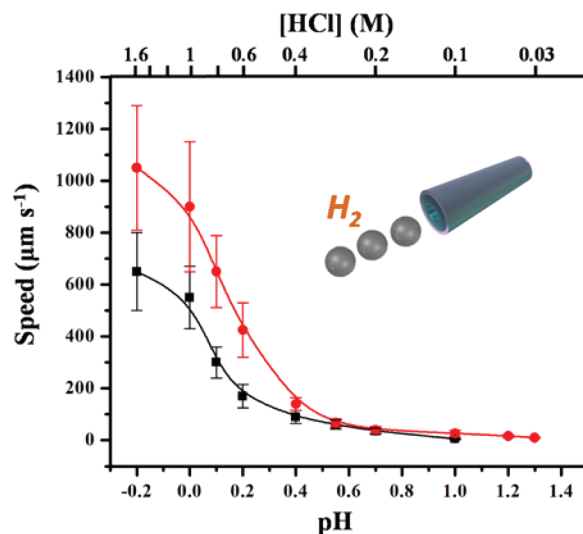
Figure 3. pH dependence of the speed of PANI/Zn microrockets in solutions of different HCl concentrations over the 0−1.6 M range. 1.67% Triton X-100 was added as the surfactant. Error bars show standard deviations of the measured speeds ($n = 30$). Red and black curves represent microrockets with 5 and 2 μm diameter, respectively.

(~100 body lengths/s) at pH −0.2, decaying gradually to 140 μm/s at pH 0.4 and then more slowly to 10 μm/s at pH 1.3. Note that such a wider operational pH range makes these rockets useful for movement in the extreme stomach environment of pH 0.8−2.0. The lifetime of the corresponding microrockets is influenced by the rate of the Zn dissolution and may range from 10 s to 2 min. This depends on both the surrounding pH (that influences the rate of the Zn dissolution) and the amount of Zn present. For example, SI Video 2 illustrates a prolonged movement of the 5 μm microrocket over 1 min in a 60 mM HCl solution (pH 1.2) at a speed of 20 μm/s. Another key factor affecting the lifetime is the thickness of the inner Zn layer. This can be used for predicting theoretically the motor lifetime using simple kinetic calculations and assuming a cylindrical microtube motor.[22] The motor's lifetime, t, is given by $\rho h/v$, where ρ and h are the density and thickness of the Zn layer, respectively, and v is the mass reaction rate, which depends on the acid concentration and corresponds to ~4.87 × 10^{-5} g/(cm^2·s) for 0.25 M H$_2$SO$_4$.[37] A lifetime of ~30 s can thus be estimated for a 5 μm diameter microrocket with a Zn-layer thickness of around 2 μm propels in 0.25 M H$_2$SO$_4$. This theoretical value is in close agreement with the experimental lifetime observed under these conditions.

The defined speed−pH profiles of Figure 3 can form the basis for sensitive motion-based pH measurements in extremely acidic environments where common glass pH electrodes lead to a large "acid error".[38,39] Microrocket-based pH sensing could involve measurements of the speed and/or distance traveled by the microrocket, analogous to a recent motion-based DNA sensing protocol.[27,40] Such motion-based pH sensing could find important applications ranging from detecting changes in the stomach acidity to remote monitoring of etching baths in semiconductor processing. Changing movement in an acid gradient (i.e., chemotaxis) can also be envisioned on the basis of the data of Figure 3.

Propulsion of the PANI/Zn microrocket in different acidic environments has also been investigated. Table 1 and corresponding SI Video 3 show the speed of the Zn-based microrockets in different common strong acids (HCl, H$_2$SO$_4$,

Table 1. Comparison of the Speed of PANI/Zn Microrockets in the Presence of Different Acids[a]

| acid	speed (μm/s)
HCl	140
H_2SO_4	80
H_3PO_4	20

[a] 0.5 M HCl, 0.25 M H_2SO_4, and 0.167 M H_3PO_4 were used along with 1.67% Triton X-100 surfactant.

and H_3PO_4). While a fast speed of 140 μm/s is observed in 0.5 M HCl, significantly slower speeds of 80 and 20 μm/s are obtained in H_2SO_4 and H_3PO_4, respectively, reflecting their decreasing acid dissociation constants.[41] Such speed variations are consistent with the pH dependence of the PANI/Zn microrocket observed in Figure 3. In contrast, no efficient propulsion was observed in a 0.5 M HNO_3 solution, although the zinc layer was dissolved. The lack of movement in nitric acid reflects the generation of N_2O (instead of H_2), which is much more soluble in water, according to

$$4Zn + 10HNO_3(\text{dilute}) \rightarrow 4Zn(NO_3)_2 + N_2O + 5H_2O \qquad (2)$$
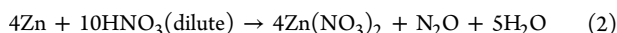
A magnetic layer can be incorporated into the PANI/Pt microrockets by E-beam deposition of Ti–Ni layers on the outer PANI surface, to allow magnetic control of their directionality and cargo pickup, as desired for practical applications of nano-/microscale machines. SI Video 4 shows a magnetically guided movement of the PANI/Zn microrocket (5 μm in diameter) in a 0.4 M hydrochloric acid at a speed of near 100 μm/s. This speed is slower than that of the PANI/Zn microrocket under the same conditions (140 μm/s), reflecting the influence of the additional Ti/Ni layers. Directed transport of cargo is important in diverse applications of micro-/nanomotors.[23,42−44] The optical images of Figure 4 and the corresponding SI Video 5 illustrate an entire cargo "load, drag, and drop" operation by the magnetically guided Ni/Ti/PANI/Zn microrocket (panels b–d, respectively) in a strong acidic environment (400 mM HCl, pH 0.4). The microrocket thus approaches the 5 μm diameter magnetic polystyrene microsphere (a), captures it magnetically (b), transports it over a predetermined path (c), and finally releases it by rapidly changing the direction the magnetic field direction (d). The speed of the microrocket decreases from 110 μm/s to 90 μm/s after capturing the polystyrene cargo, reflecting the increased fluid drag force exerted by the larger largo. A drag force of ∼5 pN can be estimated by considering the microrocket as a cylindrical nanorod.[22,29] Direct locomotion in untreated biological environments has also been illustrated. SI Video 6 shows the movement of the H_2-bubble-propelled PANI/Zn microrocket in acidified human serum over a 5 s period. Despite the raw biological medium, the PANI/Zn microrocket moves rapidly, yet at a slower speed of 92 μm/s compared to 170 μm/s in the aqueous acid solution. The higher viscosity of the human serum leads to a larger size and lower frequency of the hydrogen bubbles, and hence to a slower speed.[29]

In conclusion, we demonstrate here the first example of microtube rockets that propel efficiently by the thrust of hydrogen bubbles in extreme acidic environments. Unlike common oxygen-bubble-propelled microengines, these mass-produced low-cost PANI/Zn microrockets are fueled by their own acid environment, without additional hydrogen peroxide. The new self-propelled microrockets display an ultrafast propulsion (as high as 100 body lengths/s) along with
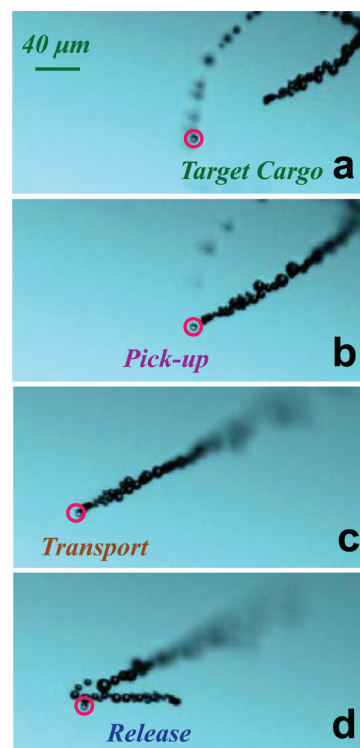
Figure 4. Cargo manipulations: time-lapse images of a PANI/Zn microrocket (5 μm diameter) approaching (a), capturing (b), transporting (c), and releasing (d) the 5 μm target sphere. Medium, 400 mM HCl solution containing 1.67% Triton X-100.

attractive capabilities ranging from guided cargo transport to propulsion in raw biological media. Such acid-powered microrockets could greatly expand the scope of applications of nano-/microscale motors toward new extreme environments (e.g., the human stomach or silicon wet-etching baths) and could thus lead to diverse new biomedical or industrial applications ranging from targeted drug delivery or nano-imaging to the monitoring of industrial processes. In addition, such self-propelled microrockets offer considerable promise for motion-based pH sensing in extreme conditions.

■ ASSOCIATED CONTENT

Ⓢ Supporting Information

Microrocket preparation, related protocols, instrumentation, reagents, additional data, and videos. This material is available free of charge via the Internet at http://pubs.acs.org.

■ AUTHOR INFORMATION

Corresponding Author
josephwang@ucsd.edu

■ ACKNOWLEDGMENTS

■ REFERENCES

(1) Paxton, W. F.; Kistler, K. C.; Olmeda, C. C.; Sen, A.; St. Angelo, S. K.; Cao, Y.; Mallouk, T. E.; Lammert, P. E.; Crespi, V. H. *J. Am. Chem. Soc.* **2004**, *126*, 13424.

(2) Fournier-Bidoz, S.; Arsenault, A. C.; Manners, I.; Ozin, G. A. *Chem. Commun.* **2005**, *4*, 441.

(3) Mallouk, T. E.; Sen, A. *Sci. Am.* **2009**, *300*, 72.

(4) Dreyfus, R.; Baudry, J.; Roper, M. L.; Ferminger, M.; Stone, H. A.; Bibette, J. *Nature* **2005**, *437*, 862.

(5) Zhang, L.; Abbott, J. J.; Dong, L. X.; Kratochvil, B. E.; Bell, D.; Nelson, B. J. *Appl. Phys. Lett.* **2009**, *94*, 64107.

(6) Gao, W.; Sattayasamitsathit, S.; Manesh, K. M.; Weihs, D.; Wang, J. *J. Am. Chem. Soc.* **2010**, *132*, 14403.

(7) Pak, O. S.; Gao, W.; Wang, J.; Lauga, E. *Soft Matter* **2011**, *7*, 8169.

(8) Loget, G.; Kuhn, A. *J. Am. Chem. Soc.* **2010**, *132*, 15918.

(9) Calvo-Marzal, P.; Sattayasamitsathit, S.; Balasubramanian, S.; Windmiller, J. R.; Dao, C.; Wang, J. *Chem. Commun.* **2010**, *46*, 1623.

(10) Pavlick, R. A.; Sengupta, S.; McFadden, T.; Zhang, H.; Sen, A. *Angew. Chem. Int. Ed.* **2011**, *50*, 9374.

(11) Hong, Y. Y.; Diaz, M.; Cordova-Figueroa, U. M.; Sen, A. *Adv. Funct. Mater.* **2009**, *20*, 1568.

(12) Zhao, G. J.; Seah, T. H.; Pumera, M. *Chem. Eur. J.* **2011**, *17*, 12020.

(13) Wang, J. *ACS Nano* **2009**, *3*, 4.

(14) Ozin, G. A.; Manners, I.; Fournier, S. B.; Arsenault, A. *Adv. Mater.* **2005**, *17*, 3011.

(15) Sanchez, S.; Pumera, M. *Chem. Asian J.* **2009**, *4*, 1402.

(16) Gibbs, J.; Zhao, Y. -P. *Appl. Phys. Lett.* **2009**, *94*, 163104.

(17) Gao, W.; Sattayasamitsathit, S.; Wang, J. *Chem. Rec.* **2011**, DOI: 10.1002/tcr.201100031.

(18) Mei, Y. F.; Solovev, A. A.; Sanchez, S.; Schmidt, O. G. *Chem. Soc. Rev.* **2011**, *40*, 2109.

(19) Mei, Y. F.; Huang, G. S.; Solovev, A. A.; Urena, E. B.; Monch, I.; Ding, F.; Reindl, T.; Fu, R. K. Y.; Chu, P. K.; Schmidt, O. G. *Adv. Mater.* **2008**, *20*, 4085.

(20) Solovev, A. A.; Mei, Y. F.; Urena, E. B.; Huang, G. S.; Schmidt, O. G. *Small* **2009**, *5*, 1688.

(21) Manesh, K. M.; Yuan, R.; Clark, M.; Kagan, D.; Balasubramanian, S.; Wang, J. *ACS Nano* **2010**, *4*, 1799.

(22) Li, J. X.; Huang, G. S.; Ye, M. M.; Li, M. L.; Liu, R.; Mei, Y. F. *Nanoscale* **2011**, *3*, 5083.

(23) Solovev, A. A.; Sanchez, S.; Pumera, M.; Mei, Y. F.; Schmidt, O. G. *Adv. Funct. Mater.* **2010**, *20*, 2430.

(24) Sanchez, S.; Solovev, A. A.; Harazim, S. M.; Schmidt, O. G. *J. Am. Chem. Soc.* **2011**, *133*, 701.

(25) Balasubramanian, S.; Kagan, D.; Hu, C. J.; Campuzano, S.; Jesus Lobo-Castañon, M.; Lim, N.; Kang, D. Y.; Zimmerman, M.; Zhang, L.; Wang, J. *Angew. Chem. Int. Ed.* **2011**, *50*, 4161.

(26) Kagan, D.; Campuzano, S.; Salasubramanian, S.; Kuralay, F.; Flechsig, G. U.; Wang, J. *Nano Lett.* **2011**, *11*, 2083.

(27) Orozco, J.; Campuzano, S.; Kagan, D.; Zhou, M.; Gao, W.; Wang, J. *Anal. Chem.* **2011**, *83*, 7962.

(28) Campuzano, S.; Kagan, D.; Orozco, J.; Wang, J. *Analyst* **2011**, *136*, 4621.

(29) Gao, W.; Sattayasamitsathit, S.; Orozo, J.; Wang, J. *J. Am. Chem. Soc.* **2011**, *133*, 11862.

(30) Liu, R.; Sen, A. *J. Am. Chem. Soc.* **2011**, *133*, 20064.

(31) Paxton, W. F.; Baker, P. T.; Kline, T. R.; Wang, Y.; Mallouk, T. E.; Sen, A. *J. Am. Chem. Soc.* **2006**, *128*, 14881.

(32) Belay, N.; Daniels, L. *Antonie van Leeuwenhoek* **1990**, *57*, 1.

(33) Yano, M.; Fujitani, S.; Nishio, K.; Akai, Y.; Kurimura, M. *J. Power Source* **1998**, *74*, 129.

(34) Funke, H. H.; Diaz, H.; Liang, X.; Carney, C. S.; Weimer, A. W.; Li, P. *Int. J. Hydrogen Energy* **2008**, *33*, 1127.

(35) Sato, Y.; Takahashi, M.; Asakura, H.; Yoshida, T.; Tada, K.; Kobayakawa, K.; Chiba, N.; Yoshida, K. *J. Power Source* **1992**, *38*, 317.

(36) Chiplonkar, S. A.; Kawade, R. *Nutrition* **2011**, DOI: 10.1016/j.nut.2011.08.019.

(37) Agrawal, Y. K.; Talati, J. D.; Shah, M. D.; Desai, M. N.; Shah, N. K. *Corros. Sci.* **2004**, *46*, 633.

(38) Kurz, J. L.; Farrar, J. M. *J. Am. Chem. Soc.* **1969**, *91*, 6057.

(39) Wang, J. *Analytical Electrochemistry*, 3rd ed.; John Wiley & Sons, Inc.: Hoboken, NJ, 2006.

(40) Wu, J.; Balasubramanian, S.; Kagan, D.; Manesh, K. M.; Campuzano, S.; Wang, J. *Nat. Commun.* **2010**, DOI: 10.1038/ncomms1035.

(41) Perrin, D. D. *Ionisation Constants of Inorganic Acids and Bases in Aqueous Solution*, 2nd ed.; Pergamon: Oxford, UK, 1982.

(42) Burdick, J.; Laocharoensuk, R.; Wheat, P. M.; Posner, J. D.; Wang, J. *J. Am. Chem. Soc.* **2008**, *130*, 8164.

(43) Sundararajan, S.; Lammert, P. E.; Zudans, A. W.; Crespi, V. H.; Sen, A. *Nano Lett.* **2008**, *8*, 1271.

(44) Kagan, D.; Laocharoensuk, R.; Zimmerman, M.; Clawson, C.; Balasubramanian, S.; Kang, D.; Bishop, D.; Sattayasamitsathit, S.; Zhang, L.; Wang, J. *Small* **2010**, *6*, 2741.